Dynamics of hydrogels with a variable ratio of permanent and transient crosslinks: constitutive model and its molecular interpretation

Jingwen Zhao, Jingyi Guo, Costantino Creton, Chung-Yuen Hui, Tetsuharu Narita

Dynamics of hydrogels with a variable ratio of permanent and transient crosslinks: constitutive model and its molecular interpretation

Jingwen Zhao[1], Jingyi Guo[2], Costantino Creton[1,3], Chung Yuen Hui[2,3], and Tetsuharu Narita[*1,3]

1 Laboratoire Sciences et Ingénierie de la Matière Molle, ESPCI Paris, PSL University, Sorbonne Université, CNRS, F-75005 Paris, France.

2 Department of Mechanical and Aerospace Engineering, Field of Theoretical and Applied Mechanics, Cornell University, Ithaca NY 14853, USA.

3 Global Station for Soft Matter, Global Institution for Collaborative Research and Education, Hokkaido University, Sapporo, Japan

Corresponding author e-mail address: tetsuharu.narita@espci.fr

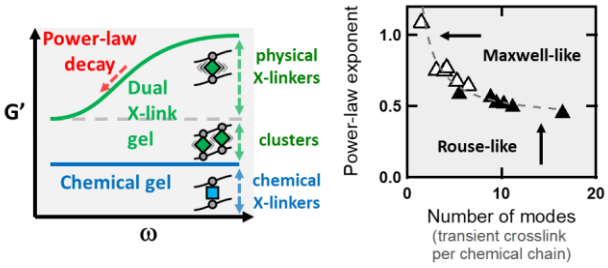

For Table of Contents use only

Abstract

Mechanical reinforcement of hydrogels is important to gel science. "Dual crosslink" hydrogels with chemical and transient crosslinks can exhibit improved mechanical properties compared to the corresponding chemically crosslinked gels. Here we use model dual poly(vinyl alcohol) crosslink gels with a variable ratio of chemical and transient crosslinks to study how this ratio affects chain dynamics. Torsion and tensile test results are well described by a constitutive model with only four parameters. The characteristic time of network relaxation (corresponding to the peak of the loss modulus) increases with decreasing transient crosslinker concentration. The characteristic time distribution gradually changes from Maxwell-like to Rouse-like relaxation. These results imply that the Rouse mode of the chains between crosslinks controls transient network dynamics. Our work provides a molecular interpretation of network dynamics and guide optimization of the crosslinking ratios in dual crosslink gels.

1. Introduction

To overcome the brittleness of conventional chemical hydrogels for applications requiring mechanical toughness, various strategies of mechanical reinforcement have been reported since 2001.[1-4] Among them, the concept of sacrificial bonds to dissipate strain energy and prevent stress concentration to the crack tip was found promising. After the pioneering works of Gong and her coworkers on "double network" hydrogels using irreversible covalent bond breaking in the interpenetrated networks,[3,5] use of reversible breaking of noncovalent bonds which can break and reform has become popular and various examples of such dissipative hydrogels having different noncovalent interactions as reversible crosslinks have been reported in the last decades.[6-10] Reversible dissociation/reassociation of the crosslinks can provide self-recovering properties to the networks, attracting the attention of material scientists.[11-13]

Though their specific time-dependent mechanical properties are of interest from a rheological point of view, quantitative studies have been less reported. The two main parameters investigated in our study are the concentration of elastically active crosslinks, which determines the modulus, and the lifetime of the transient crosslinks, which controls the network relaxation time. While it is feasible to tailor transient crosslinks at the molecular scale by choosing their concentration and their lifetime by picking various types of interactions, it is more difficult to quantitatively correlate molecular parameters to macromolecular properties such as the distribution of chain relaxation times. In addition, it is a challenge to design and synthesize a simple model dissipative gel system and to develop constitutive models able to quantitatively describe the mechanical behaviors under small and large deformations with different loading histories by taking into account the transient bond dynamics, with as few parameters as possible.

Narita, Creton and their coworkers have developed a simple model dynamic hydrogel based on poly(vinyl alcohol), PVA, having simultaneously chemical and physical crosslinks.[14-17]

Starting from a PVA chemical gel crosslinked by glutaraldehyde, a "dual crosslink" PVA hydrogel is prepared by immersing the chemical gel into a solution of borax to incorporate borate ions acting as physical crosslinkers. When the stretch rate is sufficiently small compared to the characteristic relaxation time of the transient crosslinks, it was demonstrated that incorporation of the transient crosslinks to the chemical network improves the fracture resistance of the gel compared to the corresponding chemical gel. The dynamics of the PVA dual crosslink gel has a well-defined main relaxation time determined from the peak of the loss modulus, stemming from the physical bond dissociation. Using the PVA dual crosslink hydrogel, some rheological features such as additivity of the physical crosslinks and chemical crosslinks (equivalent to the corresponding chemical gel) in terms of the moduli, as well as separability of the strain rate-dependent stress into a time-dependent term and a strain-dependent term (expressed as a neo-Hookean model), have been experimentally demonstrated (for certain loading histories).[14,15]

Hui and Long proposed a 3D finite strain constitutive model for the PVA dual crosslink gel.[18-20] A simplified description of the dynamics of the transient physical crosslinks with breaking and healing times, taking into account the steady-state behavior of the transient physical crosslinks, can fit both uniaxial tensile tests and torsion tests in shear rheometry. Using only four physically grounded parameters, the model can fit and predict very well various loading/unloading behaviors at different stretch rates. The model was successfully used to model the propagation of a crack in the PVA dual crosslink gel.[17,21]

In these previous works, the mechanical properties of the PVA dual crosslink gel were intensively studied at one preparation condition at a fixed chemical and physical crosslinkers concentrations, optimized for high toughness. The constitutive model has been applied to the same optimized gel. It is however interesting to investigate the effects of the two main parameters controlling transient crosslinks, their concentration and the relaxation time. The

effect of the relaxation time was investigated as a function of the temperature for the optimized gel.[22] The validity of the model and the applicability of time-temperature superposition were confirmed. Here we report the influence of the relative ratio of chemical and physical crosslinks on the rheological properties. We investigate a series of PVA dual crosslink gels with different ratios of permanent and transient crosslinks. All gels are characterized by uniaxial tensile tests and torsion tests and the validity of the constitutive model is tested by fitting both tensile and torsion results with the same set of two parameters for the moduli and another two for the characteristic time. More importantly, analyzing the crosslinker concentration dependence of the parameters also helps us to understand their physical significance. A goal of this paper is to provide molecular interpretations of the model parameters.

2. Experimental Section

2.1. Sample preparation

PVA dual crosslink gel samples at different chemical and physical crosslinking ratios were prepared by using the procedure described previously.[15,16] Briefly, PVA chemical gels were first prepared by cross-linking PVA (molecular weight: 89,000–98,000, degree of hydrolyzation: 99 %) in aqueous solutions with the chemical crosslinker glutaraldehyde, GA, at pH =1.9. The PVA concentration was kept constant at 12 wt% for all the gels tested. We used two GA concentrations in the feed, 5.5 and 16.5 mM, corresponding to crosslinking ratio in the feed, C_{GA} = 0.2 and 0.6 mol% (molar ratio to the monomer units of PVA). After the overnight crosslinking reaction, the obtained PVA chemical gels were used for measurements as prepared. PVA dual crosslink gels were then prepared by incorporating borate ions, physical crosslinkers, to the chemical gels. In this process the chemical gels were washed with a large amount of water to a neutral pH. The swollen chemical gels were then immersed in aqueous solutions of sodium tetraborate decahydrate (borax) for 3 days. The borax concentration in the solution, C_{borax}, varied from 1 to 50 mM. The volume of the borax solution was 20 times that of the chemical gels. By dissolution of tetraborate, borate ions are formed, which are able to form complexes with diols on the PVA chains. To quantitatively study the effects of the physical crosslinking ratio, it is crucial to compare gels with different crosslinking ratios at the same PVA concentration. It should be noted that the complexation of borate ions induces both deswelling (due to crosslinking) and swelling (due to the introduction of charges to the neutral gel). The swelling ratio was controlled by addition of NaCl to the system: the electrostatic interactions are screened and the gels deswell to the same PVA concentration as that of the corresponding chemical gel. For each GA and borax concentration, the optimal NaCl concentration was determined and varied from 90 to 460 mM.[16]

2.2. Mechanical tests

2.2.1. Tensile tests

Stress relaxation in uniaxial tensile tests was performed on an Instron 5565 tensile tester with a 10 N load cell. Samples of dual crosslink gels as well as chemical gels in a rectangular shape with 5 mm width, 1.5 mm thickness, and 20 mm gauge length (length between clamps) were stretched to $\lambda_0 = 1.1$ at a constant stretch rate of 0.1 s^{-1}, then stress relaxation was recorded. We kept the samples in paraffin oil during all the tests to prevent them from drying.

2.2.2. Torsion tests

To characterize the linear viscoelastic properties of the dual crosslink gels and the chemical gels, small strain oscillatory shear measurements were performed on a parallel plate geometry having roughened surfaces (25 mm in diameter) with an ARES LS1 rheometer (TA instruments). The sample thickness was 1.5 mm. Frequency sweep tests with a dynamic range varying from 0.1 to 100 rad/s were carried out at 25 °C within the linear viscoelasticity regime (0.8 – 1 % strain).

3. Continuum theory

3.1. Model description

Here we briefly describe the latest version of the rate-dependent finite three-dimensional continuum theory validated in the Gaussian chain regime for stretch lower than about 2, with a PVA dual crosslink gel having a chemical crosslinking ratio of 0.2 mol% prepared with C_{borax} of 1 mM.[20,22] This model was developed with the following key assumptions. (1) The chemical crosslinks are assumed to be unbreakable (fracture is not considered) while the physical crosslinks are assumed to undergo a time-dependent breaking and reforming (healing) process. The dual crosslink gel network consists of permanent chains attached to chemical crosslinks and transient chains attached to physical crosslinks. The strain energy of the network is thus the sum of that of the permanent and transient chains. (2) The physical bonds' breaking and reforming process reaches a dynamic equilibrium soon after the gel is synthesized. In other word, there is a thermodynamic equilibrium between "closed" transient crosslinks (elastically active) and "open" crosslinks. Thus, the molar fraction of breaking crosslinks and healed crosslinks per unit time are equal and independent of time (steady state assumption). This breaking (healing) rate is denoted by $\bar{\gamma}_{\infty}$ (s^{-1}). (3) The stress sustained by a transient chain is instantaneously relaxed when it breaks; after a temporary chain is reattached, it is in the relaxed state immediately and carries no strain energy. The reattached temporary chain experiences the deformation history from its birth at time τ (s) to the current time t (s). (4) Macroscopically the gel is incompressible and isotropic. For both permanent and transient chains, the Neo-Hookean model (Gaussian chains) is used to specify the strain energy of a chain under deformation. (5) We assume that the rates of chain breaking and healing are independent of the imposed strain history as observed by experiments.[15]

Assuming that before loading ($t < 0$), the physical crosslinks have reached a state of dynamic equilibrium in which the healing rate is equal to the breaking rate, i.e., $\bar{\gamma}_\infty$, the nominal stress σ (Pa) in a uniaxial tension test with stretch ratio $\lambda(t)$ is:

$$\sigma = \mu\rho\left(\lambda(t) - \frac{1}{\lambda^2(t)}\right) + \mu n(t)\left(\lambda(t) - \frac{1}{\lambda^2(t)}\right) + \mu\bar{\gamma}_\infty \int_0^t \phi_B\left(\frac{t-\tau}{t_B}\right)\left(\frac{\lambda(t)}{\lambda^2(\tau)} - \frac{\lambda(\tau)}{\lambda^2(t)}\right) d\tau. \quad \textbf{(eq.1)}$$

Equation (1) means that the stress is the sum of three terms: (i) the stress carried by the permanent network (the first term of the right side), (ii) the stress carried by the transient chains existing from $t = 0$ (the second term) and survives to the current time, (iii) and the stress carried by healed transient chains (the third term with the integral).

The use of neo-Hookean model means that the stress in the permanent network is $\mu\rho\left(\lambda(t) - \frac{1}{\lambda^2(t)}\right)$, where μ (Pa) is the small stain shear modulus, ρ is the molar fraction of the permanent chains relative to the total number of chains. Since both the transient and permanent networks obey Gaussian chain statistics (i.e., neo-Hookean model) the stress carried by the transient chains has the same dependence on the stretch ratio except in this case ρ is replaced by the molar fraction of the transient crosslinks, which are attached at $t = 0$ and survive to the current time $t > 0$, $n(t)$. $n(t)$ is[19,20]

$$n(t) = \bar{\gamma}_\infty \int_{-\infty}^{0} \phi_B\left(\frac{t-\tau}{t_B}\right) d\tau = \bar{\gamma}_\infty \frac{t_B}{2-\alpha_B}\left[1 + (\alpha_B - 1)\frac{t}{t_B}\right]^{\frac{2-\alpha_B}{1-\alpha_B}}, \quad \textbf{(eq.2)}$$

where $\bar{\gamma}_\infty$ (s^{-1}) and ϕ_B are given by

$$\bar{\gamma}_\infty = \frac{1-\rho}{t_H + \frac{t_B}{2-\alpha_B}}, \quad \textbf{(eq.3)}$$

$$\phi_B\left(\frac{t-\tau}{t_B}\right) = \left[1 + (\alpha_B - 1)\frac{t-\tau}{t_B}\right]^{\frac{1}{1-\alpha_B}}. \quad \textbf{(eq.4)}$$

$\bar{\gamma}_\infty$ (s^{-1}) is a function of the characteristic transient bond breaking time t_B (s) and the characteristic transient bond healing time t_H (s). Its physical signification can be better explained by shear modulus expression shown later in this section. $\phi_B(t-\tau)$ is called the survivability function which denotes the fraction of chains that are born at τ and survive till the current time $t > \tau$. Eg.4 can be obtained by solving a simple breaking model, $d\phi_B/dt = -\phi_B^{\alpha_B}/t_B$, where $1 < \alpha_B < 2$ is a dimensionless material constant that specifies the average survival time of a physical bond, to statistically describe the spectrum of the relaxation time related to the transient physical bond breaking. This second term represent the stress relaxation due to the breaking of the physical bonds attached at $t = 0$.

The third term expresses the recovery of stress by healing of the broken bonds. We assume that the transient chain healed at $t = \tau$ does not carry stress, starts to obey the same survivability function ϕ_B, and has a different reference configuration from the original chain. This results in a different stretch dependent term $\lambda(t)\cdot\lambda^{-2}(\tau) - \lambda(\tau)\cdot\lambda^{-2}(t)$.

The theory also predicts the dynamic shear modulus in linear viscoelastic regime with the same set of parameters.[19,22] The complex modulus $G^*(\omega)$ is written as:

$$G^*(\omega) = \mu\left\{\rho + \bar{\gamma}_\infty \frac{t_B}{2-\alpha_B}\left[1 - \frac{2-\alpha_B}{\alpha_B - 1}\cdot I(\omega)\right]\right\} \quad \textbf{(eq.5)}$$

with

$$I(\omega) = \int_0^\infty exp\left(-i\frac{\omega t_B}{\alpha_B - 1}u\right)(1+u)^{-\frac{1}{\alpha_B - 1}}\cdot du \quad \textbf{(eq.6)}$$

The integral $I(\omega)$ which is a function of the angular frequency ω, is numerically evaluated. And the expressions for $G'(\omega)$ and $G''(\omega)$ are given as:

$$G'(\omega) = Re[G^*(\omega)]$$

$$= \mu\rho + \mu\bar{\gamma}_\infty \frac{t_B}{2-\alpha_B}\left[1 - \frac{2-\alpha_B}{\alpha_B - 1}\int_0^\infty cos\left(\frac{\omega t_B}{\alpha_B - 1}u\right)(1+u)^{\frac{-1}{\alpha_B - 1}}du\right] \quad \textbf{(eq.7)}$$

$$G''(\omega) = Im[G^*(\omega)]$$

$$= \mu\bar{\gamma}_\infty \frac{t_B}{2-\alpha_B}\left[\frac{2-\alpha_B}{\alpha_B - 1}\int_0^\infty sin\left(\frac{\omega t_B}{\alpha_B - 1}u\right)(1+u)^{\frac{-1}{\alpha_B - 1}}du\right] \quad \textbf{(eq.8)}$$

From **eq.7** the low frequency limit is:

$$G'(\omega \to 0)$$

$$= G_0 = \mu\rho + \left[\frac{\mu(1-\rho)t_B}{(2-\alpha_B)t_H + t_B}\Gamma\left(\frac{2\alpha_B - 3}{\alpha_B - 1}\right)cos\left(\frac{2-\alpha_B}{2(\alpha_B - 1)}\pi\right)\right]\left(\frac{t_B\omega}{\alpha_B - 1}\right)^{\frac{2-\alpha_B}{\alpha_B - 1}}$$

$$\sim \mu\rho \quad \textbf{(eq.9)}$$

In the low frequency limit, the transient chains fully relax, and the modulus corresponds to that of the permanent chains.

In the high frequency limit, we have:

$$G'(\omega \to \infty) = G_\infty$$

$$= \mu\rho + \frac{\mu(1-\rho)t_B}{(2-\alpha_B)t_H + t_B}\left[1 - \frac{(2-\alpha_B)(\alpha_B - 1)}{{t_B}^2}\frac{1}{\omega^2}\right]$$

$$= \mu\rho + \mu(1-\rho)\frac{\frac{t_B}{2-\alpha_B}}{t_H + \frac{t_B}{2-\alpha_B}}$$

$$= \mu\rho + \mu\bar{\gamma}_\infty \frac{t_B}{2-\alpha_B} \quad \textbf{(eq.10)}$$

In the high frequency limit, both permanent crosslinks and closed transient crosslinks additively contribute to the elasticity, thus the modulus corresponding to the closed transient crosslinks is written as $G'_{\text{closed}} = \mu\bar{\gamma}_\infty \frac{t_B}{2-\alpha_B}$. The fraction of closed transient crosslinks to the total

crosslinks is written as $\rho_{closed} = \bar{\gamma}_\infty \frac{t_B}{2-\alpha_B}$, since $G'_{\text{closed}} = \mu\rho_{\text{closed}}$. It should be noted that the fraction of the (total) transient crosslinks is $1-\rho$, which is equal to $\bar{\gamma}_\infty \left(t_H + \frac{t_B}{2-\alpha_B}\right) = \bar{\gamma}_\infty t_H + \rho_{\text{closed}}$ by **eq.3**. Thus, the fraction of the open transient crosslinks, ρ_{open}, is $\rho_{\text{open}} = \bar{\gamma}_\infty t_H$.

Eq.8 shows that $G''(\omega)$ is concave downward, thus the value of time, $\tau_X = 1/\omega_X$ corresponding to the maximum, which traditionally used in the interpretation of linear rheological experiments to define the relaxation time, is a reasonable characteristic time of the dissipation of the system. Its value can be analytically calculated as a function of the model parameters (the derivation is given in Supporting Information):

$$\tau_X = \frac{t_B}{(\alpha_B - 1) \cdot f\left(\frac{2-\alpha_B}{\alpha_B - 1}\right)} \qquad \textbf{(eq.11)}$$

where f is a dimensionless function of $\frac{2-\alpha_B}{\alpha_B-1}$. Therefore, τ_X is proportional to t_B, with a coefficient which is a function of only α_B. For $0.1 \leq \frac{2-\alpha_B}{\alpha_B-1} \leq 0.9$, $f\left(\frac{2-\alpha_B}{\alpha_B-1}\right)$ can be well approximated by a linear function, $f\left(\frac{2-\alpha_B}{\alpha_B-1}\right) = -0.053 + 0.802\frac{2-\alpha_B}{\alpha_B-1}$.

The five material parameters, μ (Pa), ρ, t_B (s), t_H (s) and α_B, can be reduced to the following four parameters, which have plausible rheological significance: $\mu\rho$ (Pa), $\mu\bar{\gamma}_\infty$ (Pa s^{-1}), t_B (s) and α_B. $\mu\rho$ and $\mu\bar{\gamma}_\infty$ represent the modulus (in the form of $\mu\bar{\gamma}_\infty \frac{t_B}{2-\alpha_B}$) for the chemical and the transient networks respectively, and their crosslinker concentration dependence will be discussed in section 4.2. t_B and α_B control the characteristic relaxation time of the network. Their dependences on the crosslinker concentrations and physical interpretation are discussed in section 4.3.

3.2. Parameter determination by fitting

The experiments reported in this work are performed in the linear regime where the strains are small. This is the regime of focus in this paper. The four parameters were determined by fitting the experimental data of both the tensile and torsion tests using the equations governing each test. A set of parameters fitting both tests was found. Determination of the parameters was done by fitting the data of a tensile stress relaxation test, and the parameters were fine-tuned to match the rheology data. Details of the fitting procedure can be found in the reference.[20] Briefly, from a single tensile stress relaxation test, consisting of a rapid stretching to $\lambda = \lambda_0$ and relaxation, $\mu\rho$ and α_B were determined from the relaxation part. Since the healed transient chains do not carry stress during relaxation, **eq.1** is simplified to:

$$\sigma(t) = \mu\rho\left(\lambda_0 - {\lambda_0}^{-2}\right) + \mu n(t)\left(\lambda_0 - {\lambda_0}^{-2}\right) \qquad \textbf{(eq.12)}$$

$$= \sigma_\infty + \left(\lambda_0 - {\lambda_0}^{-2}\right) \cdot \mu\bar{\gamma}_\infty \frac{t_B}{2-\alpha_B}\left[1 + (\alpha_B - 1)\frac{t}{t_B}\right]^{-\frac{2-\alpha_B}{\alpha_B - 1}}$$

where σ_∞ is the stress at long times, from which the value of $\mu\rho$ is determined as $\mu\rho = \sigma_\infty/\left(\lambda_0 - {\lambda_0}^{-2}\right)$. For $t >> t_B$, one finds from **eq.12** $\sigma(t) - \sigma_\infty \sim t^{-\frac{2-\alpha_B}{\alpha_B - 1}}$. This allows us to determine α_B from the slope of the logarithmic plot of stress versus time. t_B and $\mu\bar{\gamma}_\infty$ were determined by fitting the rapid stretching part of the stress-strain curve with **eq.1**. Next, we fitted the torsion data. $G'(\omega)$ and $G''(\omega)$ were fitted using **eq.7** and **eq.8** to fine-tune the parameters. The value of t_B was accurately determined by this fine-tuning, thanks to the peak position in G'' which is sensitive to the value of t_B (**eq.11**).

As noted in our previous work,[16] the moduli from the torsion tests are lower than those predicted from the parameters by the tensile tests by a factor of about 2. This discrepancy is believed to arise from the fact that the torsion test is performed in a parallel plate geometry (not in the cone plate geometry) where pre-compression is applied, and this is not accounted for in our equations (**eq.7** and **eq.8**).[19]

4. Results and Discussion

4.1. Fitted material parameters

A set of the fitting parameters for both the tensile and torsion tests was determined and summarized in **Table I**. Comparison between fitting curves calculated with these parameters and the experimental results of the tensile stress relaxation and the torsion frequency sweep tests are shown in **Figures 1** for four dual crosslink gels as example. In Supporting Information one can find comparisons for all the dual crosslink gels tested in this work for both tests, up to 100 s in stress relaxation tests (**Figures S2 – S5**). The model agrees well with the experimental results for all samples tested, and one set of the parameters for each dual crosslink gel can reasonably fit both tensile and torsion tests. This result indicates the validity of the model for a wide range of crosslinking ratios.

Table I. Four reduced fitting parameters and the shift factor for moduli.

C_{GA}	C_{borax}	$\mu\bar{\gamma}_\infty$	$\mu\rho$	t_B	α_B	Shift factor
(mol%)	**(mM)**	**(kPa s^{-1})**	**(kPa)**	**(s)**		
0.2	**1**	20.9	2.41	0.367	1.64	0.90
	3	77.7	3.24	0.213	1.69	0.34
	5	125	6.73	0.174	1.66	0.47
	10	263	7.82	0.110	1.67	0.48
	20	452	9.55	0.0734	1.66	0.29
	50	1240	34.9	0.0572	1.63	0.20
0.6	**1**	33.7	17.2	0.393	1.48	0.48
	3	106	19.1	0.238	1.57	0.54
	5	155	19.7	0.213	1.57	0.37
	10	340	20.9	0.130	1.60	0.41
	20	578	21.0	0.0916	1.61	0.43
	50	1020	38.4	0.0683	1.57	0.39

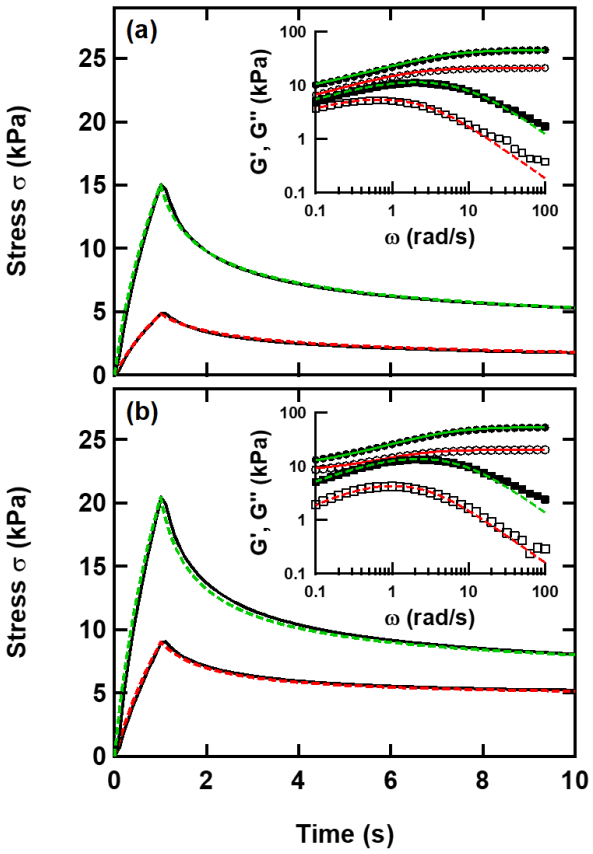

Figure 1. Comparison of the model prediction with the experimental results for the tensile relaxation tests. Uniaxial tensile stress as a function of time for dual crosslink gels with a chemical crosslinker concentration of (a) 0.2 and (b) 0.6 mol%. Results for two borax concentrations are shown, 1 mM (red) and 10 mM (green). Solid curves: experiments. Dashed curves: model prediction. Inset: Comparison of the model prediction with the experimental results for the small amplitude shear torsion tests. Viscoelastic moduli as a function of angular frequency for dual crosslink gels with a chemical crosslinker concentration of (a) 0.2 and (b) 0.6 mol%. Results for two borax concentrations are shown, 1 mM (red lines, open symbols) and 10 mM (green lines, filled symbols). Solid curves and circles: *G*'. Dashed curves and squares: *G*".

We emphasize that by fitting both tensile and torsion data, we were able to obtain reasonably accurate material parameters, for the following reasons. By fitting the tensile tests, from the stress relaxation part, the values of $\mu\rho$ and α_B can be accurately determined, while those of t_B and $\mu\bar{\gamma}_\infty$, are less accurately found (the product of them is accurately found). This is due to the relatively low amount of broken and healed transient bonds during the rapid loading phase of the relaxation test where $\dot{\lambda}$ is high but the final stretch ratio λ_0 is low. By fitting the torsion

tests, the values of t_B can be accurately determined from the peak of G''. However, the values of μρ and $\mu\bar{\gamma}_\infty$ are less accurately measured due to the precompression applied in the parallel plate geometry. The values of the shift factor used to adjust the discrepancy in the absolute values of the moduli in the tensile tests and rheology tests are also shown in **Table I**. The values of μρ and $\mu\bar{\gamma}_\infty$, which fitted well the tensile tests data, were multiplied by this factor to fit the torsion test data. The average value of these shift factors is 0.45. The dispersion of the shift factor is large since for each gel the measurement is different, and the normal force relaxation of the pre-compressed sample is difficult to control.

4.2. Modulus (μρ and $\mu\bar{\gamma}_\infty$)

4.2.1. Elastically active crosslinker populations

In this section we study the relation between the crosslinker concentrations and the two parameters, μρ and $\mu\bar{\gamma}_\infty$. We use the glutaraldehyde concentration in the feed, C_{GA} in mol%, and the borax concentration in the feed in the preparation solution, C_{borax} in mM, as experimental parameters of the chemical and physical crosslinkers concentrations, respectively. First we investigate $\mu\bar{\gamma}_\infty$. The contribution of the closed transient crosslinks to the elastic modulus is given by $G'_{\text{closed}} = \mu\bar{\gamma}_\infty \cdot \frac{t_B}{2-\alpha_B}$, which is a measurable rheological quantity of the system(recall G'_{closed} is the contribution of the phydical crosslinks to the elastic modulus at high frequency $\omega \to \infty$, see **eq.10**). Here we evaluate this reduced parameter $\mu\bar{\gamma}_\infty \cdot \frac{t_B}{2-\alpha_B}$ without discussing separately the four parameters of which it is composed (μ, $\bar{\gamma}_\infty$, t_B and α_B). The dependence of G'_{closed} on the borax concentration C_{borax} are plotted in **Figure 2a**. They increase with borax concentration, and practically no chemical crosslinker concentration dependence is found. A power-law fitting curve is shown in the figure: the exponent is found to be about 0.5, i.e., $G'_{closed} \propto C_{borax}^{0.5}$.

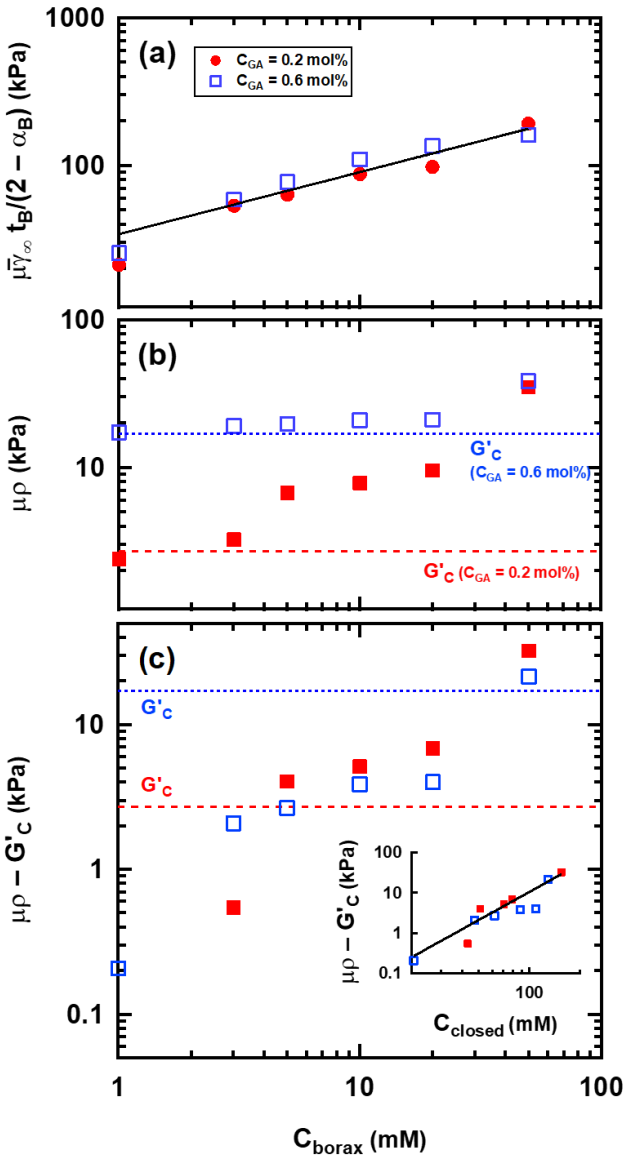

Figure 2. (a) Borax concentration dependence of $G'_{closed} = \mu\bar{\gamma}_\infty \frac{t_B}{2-\alpha_B}$ (Modulus contribution from closed transient crosslinks). The solid line is a power-law fit with an exponent of 0.51. (b) The borax concentration dependence of μρ. The dashed lines indicate the elastic modulus of the corresponding chemical gels. (c) The value of G'_{slow} = μρ – G'_C as a function of the borax concentration C_{borax} in feed. Inset: the elastically active closed physical crosslinker concentration C_{closed}. The solid line is a linear fit with an exponent of 2.3. The filled red circles represent the dual crosslink gel for C_{GA} = 0.2 mol%, open blue circles for C_{GA} = 0.6 mol%.

For a more quantitative discussion, we estimate *the molar concentration of the elastically active transient physical crosslinks*, C_{closed}, from the elastic modulus G'_{closed}. The elastic modulus is proportional to the molar concentration of elastically active chain and is written as $G'_{closed} =$

$\frac{1}{2} C_{\text{closed}} \cdot RT$, where R is the gas constant and T is the absolute temperature. The factor 1/2 indicates that each crosslinker is tetrafunctional and crosslinks two chains. In this relation C_{closed} has mol/m^3 as unit, and is recalculated in mM. We found values between 17 and 155 mM with the same C_{borax} dependence as G'_{closed}.[23]

Next we study the dependence on the borax concentration of the time-independent reduced parameter μρ. Recall that μρ corresponds to the elastic modulus at zero frequency ($t >> t_B$) (**eq.10**). We performed tensile stress relaxation test up to 100 s for t_B lower than 1 s. The physical model of the dual crosslink gel assumes that the transient crosslinks dissociate and the chains fully relax at low frequency, thus the value of μρ is expected to be the same as the modulus of the chemical gel used to prepare the dual crosslink gels, and therefore should be independent of the borax concentration in the feed, C_{borax}.

Figure 2b shows the borax concentration dependence of μρ. For both chemical crosslinking ratios, the values of the elastic modulus G'_C for the corresponding chemical gels (measured independently with the chemical gel samples) are indicated by the dashed lines. For the gels with C_{GA} = 0.2 mol%, at low borax concentrations we find fitted values of μρ close to that of the chemical gel (2.7 kPa), then they increase with increasing borax concentration. At C_{borax} = 50 mM, μρ reaches 25 kPa. For gels with C_{GA} = 0.6 mol%, at borax concentrations below 20 mM the values of μρ are comparable to that of the chemical gel (17 kPa), then they increase to 30 kPa for C_{borax} = 50 mM. These results indicate that at the lower frequency experimentally investigated, the modulus of the dual crosslink gels matches with that of the chemical gels only at sufficiently low borax concentration. *This result suggests that at high borax concentrations the physical crosslinkers increase* μρ, *forming a second population of elastically active physical crosslinkers with a much longer lifetime than that corresponding to* G'_{closed}. This second

population is rheologically indistinguishable from the chemical crosslinks within the window of observation times explored here.

The modulus due to the presence of this longer lived population of physical crosslinks can be determined by subtracting *the elastic modulus of the corresponding chemical gel* G'_C from the fitted value of $\mu\rho$ for each dual crosslink gels assuming that additivity holds for this population. The result is shown in **Figure 2c**. Even though the eventual errors of this subtraction between the data from two separate rheological measurements can be large, one can still see that the values of $G'_{slow} = \mu\rho - G'_C$ increase with borax concentration C_{borax}, and no clear effect of the degree of chemical crosslinking is found. This result suggests that the presence of the permanent crosslinks does not influence the formation of this slower population at the studied crosslinking ratios. The values of G'_{slow} (0.1 – 30 kPa) are comparable to (or lower than) those of G'_C (3 or 17 kPa). Finally, these values of modulus due to slow physical crosslinks are also lower than those of the closed physical crosslinks (21 – 190 kPa, as shown in **Figure 2a**).

To better characterize the origin of this long lived population of physical crosslinks, the values of $G'_{slow} = \mu\rho - G'_C$ are plotted in the inset of **Figure 2c** as a function of the concentration of elastically active chains due to physical crosslinkers which dissociate within the experimental time scale, C_{closed}. The values of G'_{slow} increase with C_{closed} with a power-law exponent of about 2.3. This power-law exponent suggests that the origin of this slow population is due to clustering of two (or more) physical crosslinkers.

In the case of binding of mobile crosslinkers which can diffuse in the network and bind on the chains, the binding potential can entropically and enthalpically vary depending on the position relative to the existing physical and chemical crosslinkers. Binding to a site very close to an existing crosslinker is preferred, as the local polymer concentration is higher. This clustering is also expected to bring an entropic gain for polymer chains.[24] The lifetime of a cluster made of several physical bonds should be longer than that of a single bond, as it is necessary to break

all the bonds for the chain to relax. Clustering involving a chemical crosslink and physical crosslinks might occur. However, it is difficult to rheologically detect such clusters, since they are not distinguishable from a simple chemical crosslink in the linear regime. Furthermore, we expect the concentration of clusters near a chemical crosslink to be very low since the concentration of the chemical crosslinks itself, C_C, estimated from the value of G'_C, is also very low compared to C_{closed}. The values of C_C are estimated to be 2 and 14 mM for C_{GA} of 0.2 and 0.6 mol%.

The slower population can be an important factor in determining gel failure under large deformation. Previously it was shown that the stretch at break of the dual crosslink gels is very sensitive to the chemical and physical crosslinking ratios, and decreases with increasing chemical and physical crosslinking ratio.[16] This is presumably due to the increase in the amount of the slower population which is expected to behave similarly to permanent crosslinks which enhance the brittleness.

The concentrations of the three different elastically *active* components are summarized here. The concentrations of permanent chemical crosslinks (C_C), and of the two populations of transient physical crosslinks, the fast one (C_{closed}) and slow one (C_{slow}), were estimated from the corresponding modulus and are plotted as a function of the borax concentration in the feed C_{borax} in **Figure 3a**. At all borax concentrations C_{borax} tested here, the values of C_{closed} are higher than those of C_{slow} and C_C, indicating that the time-dependent elasticity of the dual crosslink gels is still governed by the transient crosslinks. At high C_{borax}, the difference between C_{closed} and C_{slow} becomes smaller.

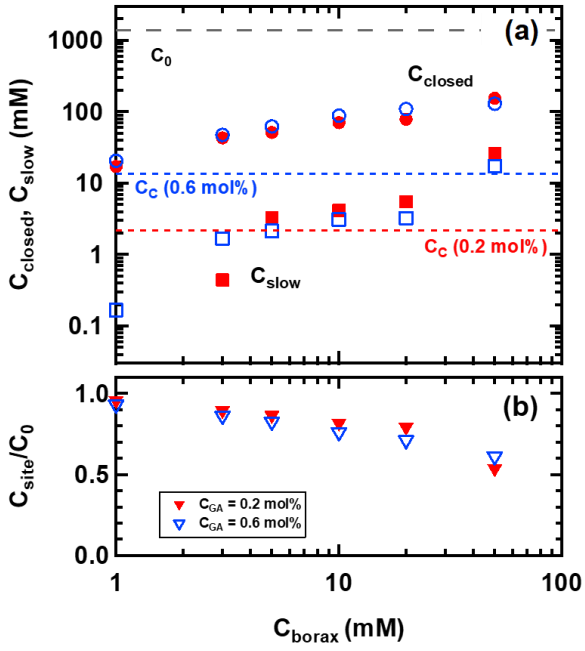

Figure 3. The borax concentrations dependence of the two populations of the transient physical crosslinks: the fast one C_{closed} (circles) and the slow one C_{slow} (squares). The red symbols are for C_{GA} = 0.2 mol%, blue ones for C_{GA} = 0.6 mol%. Dashed lines: red for *C*c for C_{GA} = 0.2 mol%, blue for *C*c for C_{GA} = 0.6 mol%, gray for the total concentration of the binding site, C_0 (see the text).

4.2.2. Elastically inactive crosslinker populations

In the previous subsection, we have shown that there are three populations of elastically active crosslinkers, and that their concentration can be estimated from the corresponding elastic modulus. The correspondence between the elastic modulus and the model parameters, μρ and $\mu\bar{\gamma}_\infty$, was also demonstrated. In our steady state model, we assume that there is a thermodynamic equilibrium between the elastically active closed crosslinks and the elastically *inactive* open crosslinks. This equilibrium depends on the physical chemistry of the dynamic bonds used as transient crosslinks. In this subsection, we discuss the open crosslinks and other elastically inactive populations of the transient crosslinks. As seen later in this subsection, the concentration of available binding sites is an important parameter influencing the dynamics of the breaking/healing of the transient crosslinks and we now attempt to approximately evaluate

it. This argument will be useful to better comprehend the discussion about the dynamics developed in the next section 4.3.

The complexation of borate ions with diol binding sites (two neighboring hydroxyl groups) on the PVA chains has two binding equilibria as borate ions can interact with one or two diol binding sites as illustrated in **Figure 4**. At equilibrium, the borate ions can take three states. (1) "Free" borate ions in the gel and in the solution which do not interact with PVA chains, their concentration is defined as C_{free} (mol/L). (2) Borate ions which complex with one diol binding site (monodiol complexation), do not crosslink chains. This state corresponds to "open" crosslink (with the concentration of C_{open}), as it readily forms a closed crosslink with an available diol binding site. (3) Borate ions complexing with two diol binding sites (didiol complexation) can be further classified into three different states which are not thermodynamically distinguishable. (3a) The borate ions in didiol complexes can be *intra*-chain didiol complexes (C_{intra}), and these complexes are elastically *inactive*. (3b) They can be also inter-chain didiol complexes which serve as "closed" crosslinks (C_{closed}), thus elastically *active*. Finally, (3c) they can also form a cluster of the didiol complexes behaving as a slow population of the crosslink (C_{slow}), considered as elastically *active*.

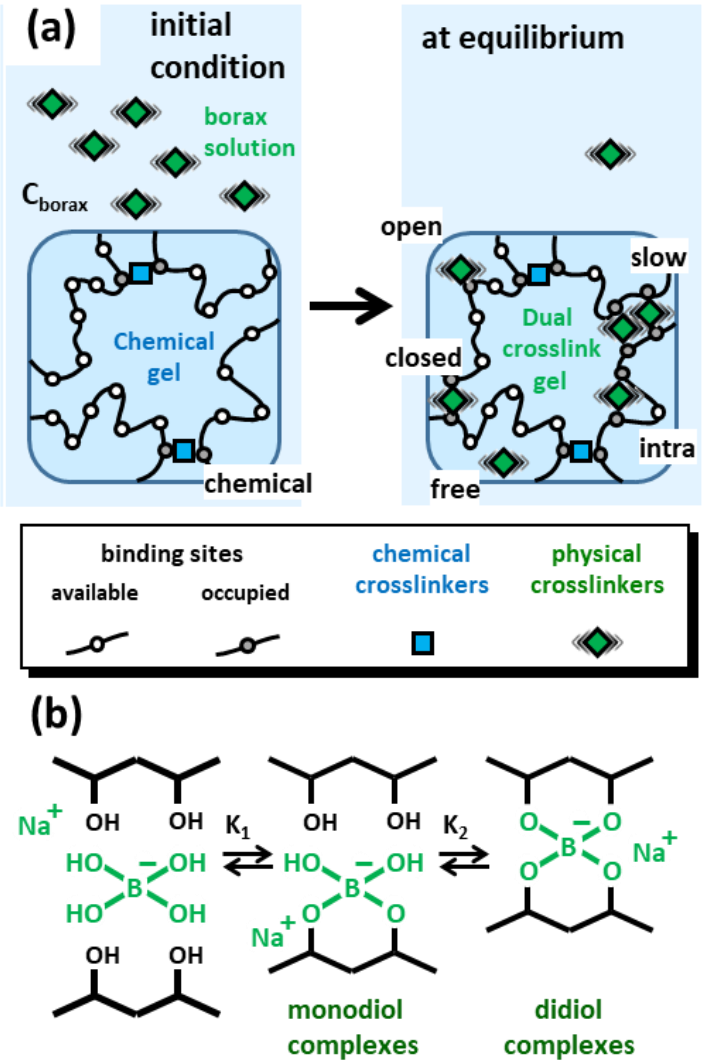

Figure 4. (a) Schematic illustrations of transient crosslinker incorporation into the chemical gel. (b) Binding equilibria of the borate ion and diols on PVA chains.

The two binding constants, K_1 and K_2 (L/mol), are written as $K_1 = \frac{C_{\text{open}}}{C_{\text{free}} \cdot C_{\text{site}}}$ and $K_2 = \frac{C_{\text{di}}}{C_{\text{open}} \cdot C_{\text{site}}}$, where C_{site} is the concentration of available binding sites on the PVA chains, and $C_{\text{di}} = C_{\text{intra}} + C_{\text{closed}} + C_{\text{slow}}$. In **Figure 5** we schematically illustrated in green these five different populations of physical crosslinkers (borate ions), as well as chemical crosslinks (in blue) and didiol binding sites on the PVA chains. For the elastically active populations (3b, 3c and the chemical crosslinks), the correspondence with $G'(\omega)$ and the model parameters are also shown. The dynamics of the transient crosslink breaking/healing are described by the second equilibrium

(i.e., by the binding constant K_2), which depends on the three concentrations, C_{di}, C_{open} and C_{site}. Here we attempt to estimate them as quantitatively as possible.

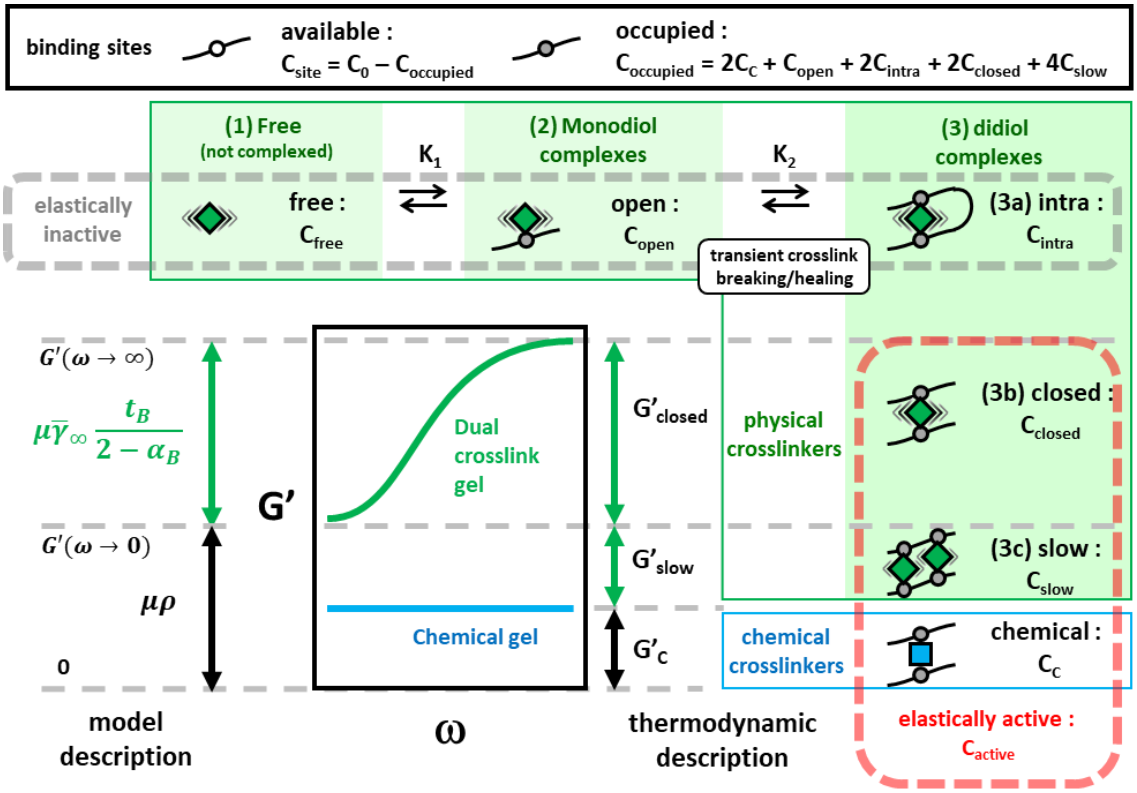

Figure 5. Classification of the different species involved in the binding equilibria of borate ion-diol complexation, and their concentration. Correspondence between the model description and the thermodynamic description of the elastic modulus.

Didiol complex concentration. Contrary to C_{closed} and C_{slow}, which are concentrations of the elastically active populations, it is experimentally difficult to determine the concentration of the rheologically undetectable intrachain crosslink, C_{intra}. In dilute solutions intrachain crosslinking is favored, while in semi-dilute solutions and gels the amount of the interchain crosslinks increases. Since intrachain crosslinking involves the formation of a loop on the polymer chain, chain rigidity is a factor controlling the size of the loop. Pezron et al.[25-27] estimated the ratio of interchain to intrachain crosslinks as a function of the polymer concentration, by correlating the sizes of the blob and the loop formed by intrachain crosslink. Applying their theory to our system with a fixed PVA concentration of 12 wt%, the ratio of inter- to intra-chain crosslink is estimated to be about 1.7. In the following, we use this value,

thus $C_{intra} = (C_{closed} + C_{slow})/1.7$. It should be noted that for our systems the PVA chains are integrated into the percolated chemical network, thus the chains between crosslinks might have lower deformability to form a loop than the chains in solution, and C_{intra} could be lower than this estimate.

Monodiol complex (open crosslink) concentration. For solutions with relatively low PVA concentrations (without chemical crosslinks), ^{11}B NMR spectroscopy has been used to determine the concentrations of different states of borate ions.[28,29] The results indicate that monodiol complexes, corresponding to open transient crosslinks have much weaker signals than the didiol complexes (closed transient crosslinks), as the binding equilibrium is toward the didiol complexes, or $C_{closed} >> C_{open}$. We will further discuss C_{open} in the next section. We did not perform NMR measurements of our chemically crosslinked systems with relatively higher PVA concentration, due to difficulties in sample preparation.

Available binding site concentration. The total concentration of binding sites is estimated to be $C_0 = 1.36$ M,[30] which is shown as a black dashed line in **Figure 3a**. The concentration of occupied binding sites can be determined from that of the chemical crosslinks and the bound borate ions in monodiol and didiol complexes, thus C_C, C_{open}, C_{closed}, C_{intra} and C_{slow}. Specifically, the concentration of the occupied sites can be written as $C_{occupied} = 2C_C + C_{open} + 2C_{closed} + 2C_{intra} + 4C_{slow}$, where the numerical factors 1, 2 or 4 in this equation indicate the number of binding sites for the different binding mechanisms and assumes a cluster of 2 didiol complexes. The concentration of available binding sites C_{site} is $C_{site} = C_0 - C_{occupied}$. The values of C_{site} are estimated by inputting into this equation the values of these different concentrations (rheologically determined: C_C, C_{closed}, C_{slow}; estimated from C_{closed} and C_{slow}: C_{intra}; C_{open} is ignored since $C_{open} << C_{closed}$). In **Figure 3b** C_{site}/C_0 is plotted as a function of the borax concentration C_{borax}. C_{site}/C_0 decreases with C_{borax}, and for the gel with the highest degree of binding, C_{site}/C_0 is estimated to be about 0.54 (C_{site} is about 0.73 M). Therefore, although the

concentration of the elastically inactive populations may not be quantitatively very accurate we can still conclude that the saturation of binding sites does not occur in the studied conditions: there are plenty of available binding sites. Note that $K_2 \cdot C_{\mathrm{site}} = \frac{C_{\mathrm{di}}}{C_{\mathrm{open}}}$, thus close to the binding saturation, with decreasing C_{site}, C_{di} relatively decreases and the dynamics of the transient crosslink breaking/healing can be very different.

4.3. Characteristic time (t_B and α_B)

In this section we investigate the effect of the crosslinking ratio on the characteristic relaxation time of the dual crosslink gels, by focusing on the two parameters, t_B and α_B. t_B is the characteristic transient bond breaking time and is proportional to the rheologically directly measurable relaxation time τ_X of the peak position of G'' (section 3.1, **eq.11**) with a coefficient depending only on α_B. In the inset of **Figure 6**, this proportionality is shown. The values of the coefficient, $1/[(\alpha_B - 1) \cdot f(q)]$, vary between 2.5 and 4.7. The concentration dependence of α_B will be discussed later in this section. As seen in the inset of **Figure 1** (and **Figure S2**), the position of the peak depends on the chemical crosslinker concentration: gels with C_{borax} = 10 mM (filled symbol, green curves) show the peak at higher frequency than the gels with C_{borax} = 1 mM (open symbols, red curves). **Figure 6** shows that fitted values of t_B obtained from the rheological curves decrease with increasing borax concentration C_{borax}, and do not show any obvious chemical crosslinking ratio dependence. The value of t_B is found to approximately scale as $t_B \sim C_{\mathrm{borax}}^{-0.48}$. Thus, for this system, the bond breaking time decreases with increasing physical crosslinker concentration.

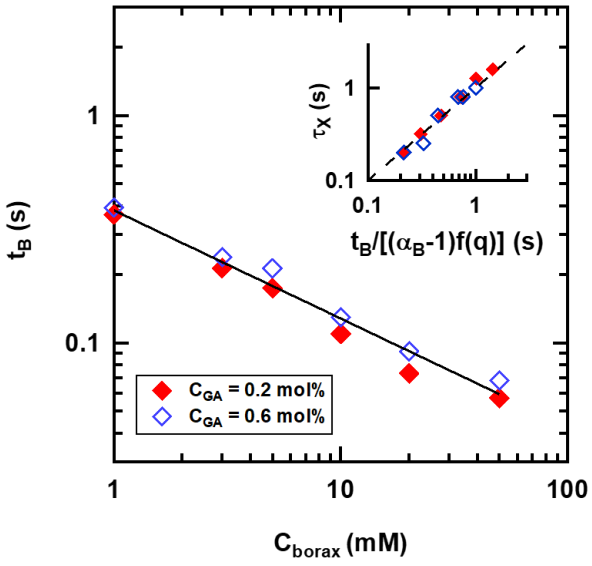

Figure 6. The values of t_B as a function of the borax concentration C_{borax}. Red diamonds: C_{GA} = 0.2 mol%; blue diamonds: C_{GA} = 0.6 mol%. The solid line is a power-law fit with an exponent of -0.48. Inset: the network relaxation time at the peak of G'', τ_X, as a function of t_B (see eq.11).

4.3.1 Molecular interpretation: theoretical framework

We now attempt to interpret this concentration (C_{borax}) dependence from a macromolecular point of view, by considering the chain relaxation dynamics as a function of transient bond breaking and healing times following the argument of Indei and Takimoto for associative polymers.[31]

In a dual crosslink network prepared from a percolated chemical network by incorporating additional transient crosslinks, each transient crosslink is located on a part of a chain between two other crosslinks which can be permanent or transient, and are elastically active during the bond breaking time scale considered here. In **Figure 7a** this chain is indicated in black and the average Kuhn segment number between two adjacent crosslinks is defined as $\bar{M}$. When the transient crosslink breaks with a characteristic breaking time t_b, a subchain having $2\bar{M}$ segments is released and starts to relax (**Figure 7b**). We will discuss the relation between this molecular parameter t_b and the model parameter t_B later in this section. The mean square displacement, MSD, of the open transient bond on this subchain (after its release) is approximately:[32]

$$MSD \sim \langle \Delta r^2 \rangle_0 \left(\frac{t}{\tau_R}\right)^{\frac{1}{2}} \quad \text{for } t < \tau_R \qquad \text{(eq.13i)}$$

$$MSD \sim \langle \Delta r^2 \rangle_0 \quad \text{for } t > \tau_R \qquad \text{(eq.13ii)}$$

where $\langle \Delta r^2 \rangle_0$ is the mean square length of the subchain, and τ_R is the Rouse relaxation time of a subchain having the segment number of $2\bar{M}$.

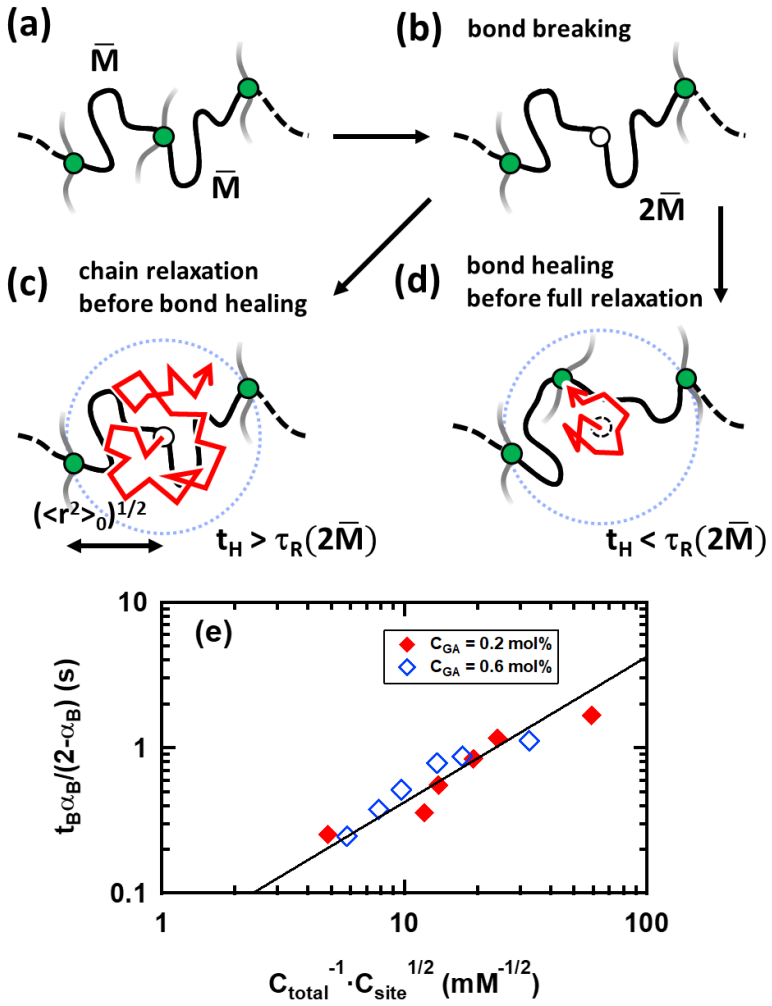

Figure 7. (a) – (d) Schematic illustrations of relaxation of a subchain after bond breaking in competition with bond healing. (e) τ_X as a function of $C_{total}^{-1} \cdot C_{site}^{1/2}$. Red diamonds: C_{GA} = 0.2 mol%; blue diamonds: C_{GA} = 0.6 mol%. The solid line is a linear fit.

Next we include bond healing in the argument: the open transient crosslink can reattach with an available binding site nearby, and its characteristic time is t_h. Since the transient crosslink

can move while it is open (starting at $t = 0$), the subchain can fully relax if $t < t_h$. Thus, we can rewrite **eq.13** by replacing t with t_h:

$$MSD \sim \langle \Delta r^2 \rangle_0 \left(\frac{t_h}{\tau_R}\right)^{\frac{1}{2}} \quad \text{for } t_h < \tau_R \qquad \textbf{(eq.14i)}$$

$$MSD \sim \langle \Delta r^2 \rangle_0 \quad \text{for } t_h > \tau_R \qquad \textbf{(eq.14ii)}$$

For the case of $t_h > \tau_R$, the subchain can fully relax before the transient crosslink reattaches (**Figure 7c**), thus the MSD of the open transient crosslink can reach its maximum value, $\langle \Delta r^2 \rangle_0$. On the contrary, for $t_h < \tau_R$, the transient crosslink reattaches before the chain fully relaxes (**Figure 7d**), thus the value of MSD is lower than that for $t_h > \tau_R$. Bond healing can occur in multiple steps (number of step: n_{step}) when $t_h < \tau_R$, until the subchain fully relaxes and its equilibrium is reached, thus $MSD \cdot n_{\text{step}} \sim \langle \Delta r^2 \rangle_0$.

The network relaxation time τ_X can also be interpreted as the time required for the subchain to reach its equilibrium state during which the transient crosslink breaks in single or multiple steps, thus it is written as

$$\tau_X \sim n_{\text{step}} \cdot t_b \sim \frac{\langle \Delta r^2 \rangle_0}{MSD} \cdot t_b \qquad \textbf{(eq.15)}$$

In summary, our analysis shows that

$$\tau_X \sim \left(\frac{\tau_R}{t_h}\right)^{\frac{1}{2}} \cdot t_b \quad \text{for } t_h < \tau_R \qquad \textbf{(eq.16i)}$$

$$\tau_X \sim t_b \quad \text{for } t_h > \tau_R \qquad \textbf{(eq.16ii)}$$

4.3.2 Molecular interpretation: Experimental data

The physical crosslinker concentration dependences of t_h and τ_R are now studied. The Rouse relaxation time of the subchain having the Kuhn segment number of $2\bar{M}$ is written as $\tau_R = \tau_0 \cdot (2\bar{M})^2$, where τ_0 is the relaxation time of the Kuhn segment. Since $\bar{M}$ is inversely proportional

to the crosslinking ratio, τ_R scales with the concentration of the total elastically active crosslinks, $C_{active} = C_{closed} + C_{slow} + C_C$, as

$$\tau_R \sim C_{\text{active}}^{-2} \quad \textbf{(eq.16iii)}$$

C_{active} is estimated from the elastic moduli, and found to be between 19 and 183 mM, For simplification, we have ignored the influence of loops made by the intrachain crosslinks on the chain dynamics. Bond healing requires an available binding site on the polymer, thus the bond reassociation time t_h is inversely proportional to its concentration, i.e.,

$$t_h \sim C_{\text{site}}^{-1} \quad \textbf{(eq.16iv)}$$

where $C_{site} = C_0 - 2C_C - C_{open} - 2C_{closed} - 2C_{intra} - 4C_{slow}$., as shown in the subsection 4.2.2. As discussed previously, we assume $C_{open} << C_{closed} < C_0$, thus we ignore C_{open}. C_{site} varies between 1.3 and 0.73 M. From **eq.16i,iii,iv**, τ_X is expected to scale as $\tau_X \sim C_{active}^{-1} \cdot C_{site}^{1/2}$. In **Figure 7e**, the values of τ_X, are plotted as a function of $C_{active}^{-1} \cdot C_{site}^{1/2}$. The solid line corresponds to a linear fit, suggesting that the scaling corresponding to **eq.16i** holds. Even at lower values of τ_X, we did not observe a regime corresponding to **eq.16ii**. The absence of this regime shows that in the studied conditions, the relaxation time of the network equals $n_{step} \cdot t_b$, with $n_{step} > 1$ and $\tau_R > t_h$.

Here we compare the constitutive model parameters (t_B and t_H) with the molecular parameters (t_b and t_h). According to the definition, t_H is identical to t_h. From **eq.11** and **eq.15**, we have $\tau_X \sim t_B \sim n_{step} \cdot t_b$. Thus we conclude that the decrease in t_B with increase in C_{borax} shown in **Figure 6** is due to the decrease in n_{step}, as a consequence of the decrease in C_{site} and of the increase in C_{active}. Since $n_{step} > 1$, it is necessary to slightly modify one of the assumptions of the model described in section 3.1 to meet the argument above. The assumption (3) should be rewritten as "(3') the stress sustained by a transient chain is relaxed with a Rouse relaxation time after single or multiple transient bond breaking steps, as a function of the healing time of

the crosslink. A fully relaxed temporary detached chain can be reattached without carrying strain energy, and experiences the deformation history from its birth at time τ (s) to the current time t (s)." The equations are identical and consistent with the argument.

Let us roughly estimate the order of the three characteristic times, τ_R, t_b, and t_h. From the value of the plateau modulus at high frequency $G' = k_B T/\xi^3$, the size of the Gaussian subchain, ξ, is determined. Then the number of Kuhn segment $\bar{M}$ is determined from $\xi = b_K \bar{M}^{1/2}$, with the Kuhn segment size of b_K. The Rouse relaxation time τ_R is written as $\tau_R = \tau_0 \cdot (2\bar{M})^2$. We used the viscosity of water, η_s = 0.00089 Pa s, b_K = 0.62 nm,[33] thus $\tau_0 = \eta_s b_K^3/k_B T = 5.2 \times 10^{-11}$ s. The values of τ_R for the dual crosslink gels studied here are estimated to be between 1×10^{-6} and 7×10^{-8} s.

The values of t_b and t_h cannot be determined from the analysis above. Still, from **eq.15** and **eq.16i**, we can estimate the highest values of t_h and t_b, as well as the lowest value of n_{step}. Specifically, since $t_h < \tau_R$, $t_b < \tau_X$, **eq.15** and **eq.16i**, imply $\tau_X/t_b \sim n_{step} = (\tau_R/t_h)^{1/2}$. Since $t_b < \tau_X$, we assume the highest value of t_b is close to the lowest value of τ_X measured, about 0.2 s. With t_b = 0.2 s, we find the values of n_{step} between 1 and 8 for the different crosslinking ratios. Since $n_{step} = (\tau_R/t_h)^{1/2}$, we can approximately estimate t_h from the values of τ_R, and we find the values of t_h is between 1×10^{-8} and 8×10^{-8} s. This very fast healing time might be due to the presence of binding site in the vicinity of the closed crosslink. In fact, practically any part of the PVA chain can be a binding site, and a dissociated crosslink can be immediately captured by a neighboring binding site.

From the thermodynamic argument,[34] we have $\frac{t_b}{t_h} = \frac{C_{\mathrm{di}}}{C_{\mathrm{open}}}$. Thus the ratio of the two characteristic time corresponds to the ratio of the closed and open crosslinks. For the largest value of t_b = 0.2, the ratio t_b/t_h varies between 3×10^6 and 2×10^7, indicating that $t_B >> t_H$ and $C_{closed} \approx C_{di} >> C_{open}$. And when t_b is smaller, then this ratio becomes larger.

4.3.3. Molecular interpretation of α_B

The values of α_B are plotted as a function of the borax concentration in **Figure 8**. For the gels with the chemical crosslinking ratio of C_{GA} = 0.6 mol%, the values of α_B are found between 1.48 and 1.61, they first increase with C_{borax} then decrease. The maximum is at C_{borax} ~ 20 mM. For gels with C_{GA} = 0.2 mol%, the values of α_B are found between 1.63 and 1.69, higher than those for the gel with C_{GA} = 0.6 mol%. Though the variation is small, they peak around C_{borax} = 3 mM.

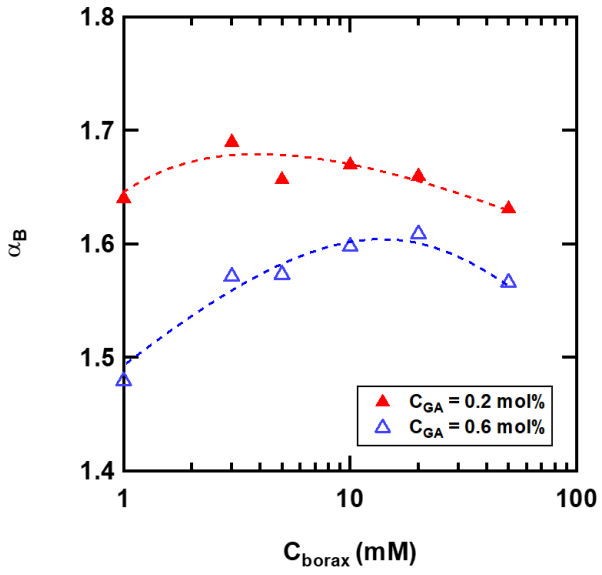

Figure 8. The values of α_B as a function of the borax concentration. Red triangles: C_{GA} = 0.2 mol%; blue triangles: C_{GA} = 0.6 mol%. The dashed curves are guide for the eye.

The material parameter α_B describes the spectrum of relaxation times of the transient strands. As shown in 4.3.1, the relaxation time τ_X depends on the subchain length, or on the crosslinking ratio. Thus it is expected that the spectrum of the relaxation times can be expressed as a function of the number of relaxation modes due to the distribution of the subchain length in the dual crosslink network. First, we find the slowest relaxation modes (longest chain). It is reasonable to take the Rouse mode of a primary chain between the two neighboring permanent crosslinks as the slowest mode, since we first prepare a permanent chemical network then we add transient

crosslinks. When the transient crosslinks are added to the primary chain, the primary chain is divided into subchains, having shorter Rouse relaxation times. We define a parameter N_P, the number of the transient crosslinks per primary chain, as the ratio of $\rho_{closed} = \bar{\gamma}_\infty \cdot \frac{t_B}{2-\alpha_B}$ to ρ, which signifies the ratio of the transient closed physical crosslinks to the permanent crosslink including the chemical crosslinks and the slow population of the physical crosslinks which do not break at the time scale of the measurement, thus behave similarly to the permanent crosslinks.

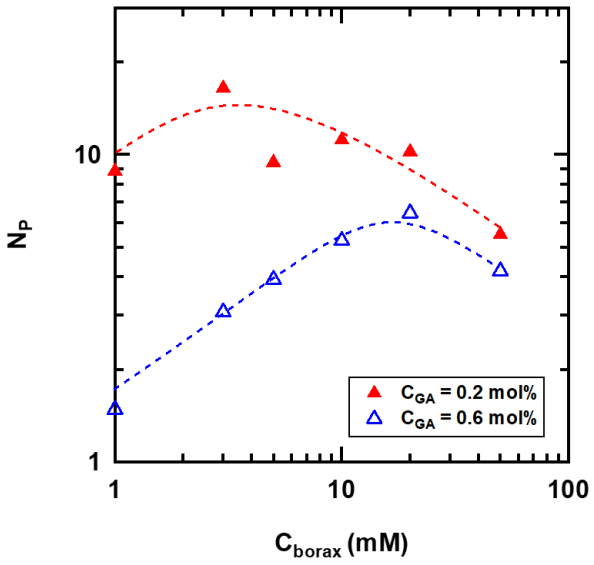

Figure 9. Number of the elastically active transient physical crosslinks per non transient crosslinks as a function of the borax concentration. Filled red triangles: C_{GA} = 0.2 mol%; open blue triangles: C_{GA} = 0.6 mol%. The dashed curves are guide for the eye.

The values of $N_P = \rho_{closed}/\rho$ are plotted as a function of C_{borax} in **Figure 9**. At low C_{borax}, N_P increases with C_{borax} as the increase in ρ_{closed} is dominant, while at high C_{borax} it decreases with C_{borax} since the increase in ρ is dominant due to the increase in the slow population of the physical crosslinks, giving a maximum. The position of the maximum is determined by the value of G'_C: for gels with the lower chemical crosslinking ratio (C_{GA} = 0.2 mol%) the peak is found at a lower C_{borax} (about 0.3 mM), while for the gels with C_{GA} = 0.6 mol% the peak is at about 20 mM. The values of N_P range between 5.5 and 16 for C_{GA} = 0.2 mol%, and between

1.5 and 6.4 for C_{GA} = 0.6 mol%, indicating that it is experimentally difficult to increase the value by more than 20 in this system.

One can notice resemblance between the C_{borax} dependence of α_B and that of N_P shown in **Figure 8** and **Figure 9**, suggesting that α_B scales with N_P. **Figure 10a** shows α_B as a function of N_P for both chemical crosslinking ratios. We clearly see a consistent trend for the two chemical crosslinker concentrations: α_B increases with N_P. This result indicates that the physical meaning of the parameter α_B is related to the number of the relaxation modes of a chain.

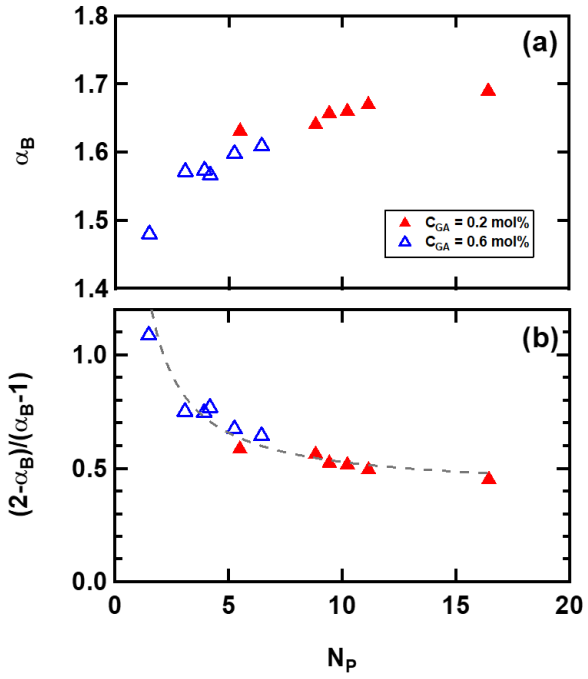

Figure 10. The values of (a) α_B and (b) $(2 - \alpha_B)/(\alpha_B - 1)$ as a function of N_P. Filled red triangles: C_{GA} = 0.2 mol%; open blue triangles: C_{GA} = 0.6 mol%. The dashed curve is an empirical relation $\frac{2-\alpha_B}{\alpha_B-1} = \frac{1.28}{N_P} + 0.40$ (see the text).

To further quantify the rheological significance of α_B, we estimate the dependence of $\frac{2-\alpha_B}{\alpha_B-1}$ on N_P. We consider the value of $\frac{2-\alpha_B}{\alpha_B-1}$ as a criterion to understand the rheological signification of α_B: in tensile relaxation tests, the power-law behavior $\sigma(t) - \sigma_\infty \sim t^{-\frac{2-\alpha_B}{\alpha_B-1}}$ is found from **eq.12**,

and in torsion tests, we find a power-law behavior $G' - \mu\rho \sim \omega^{\frac{2-\alpha_B}{\alpha_B-1}}$ from **eq.9**. The values of $\frac{2-\alpha_B}{\alpha_B-1}$ are plotted as a function of N_P in **Figure 10b**. They range between 1.09 and 0.45 and decreases with N_P. This result suggests that with increasing number of transient crosslinkers and hence relaxation modes, the dynamics of the system gradually move from a Maxwell-like behavior with $\frac{2-\alpha_B}{\alpha_B-1} = 1$ to a Rouse-like behavior with $\frac{2-\alpha_B}{\alpha_B-1} = 0.5$. It suggests also that the value of α_B can be determined from the rheologically measurable value of $N_P = \left(\mu\bar{\gamma}_\infty \cdot \frac{t_B}{2-\alpha_B}\right)/\mu\rho = [G'(\omega \to \infty) - G'(\omega \to 0)]/G'(\omega \to 0)$. By fitting the data in **Figure 10b**, we propose an empirical relation:

$$\frac{2-\alpha_B}{\alpha_B-1} = \frac{1.28}{N_P} + 0.40, \qquad \textbf{(eq.17)}$$

which is shown in the figure as a gray dashed curve. The value of $\frac{2-\alpha_B}{\alpha_B-1}$ goes to 0.4 at $N_P >> 1$, this value is slightly lower than what is expected for the Rouse mode. The two factors (1.28 and 0.40) should be intrinsic to this system. Universality of this relation needs to be further confirmed with different dual crosslink networks.

It should be noted that it is difficult to observe this Rouse-like mode in associative polymer solutions (physical gels) with small numbers of stickers (small N_P), due to the terminal flow. In fact, this Rouse-like mode should occur between the relaxation times due to the transient crosslink breaking τ_X and the terminal time $\tau_{terminal}$, where $\tau_{terminal}$ scales as $\tau_{\mathrm{terminal}} \sim \tau_X \cdot {N_P}^{2}$.[31] Thus, for small N_P, the terminal flow occurs immediately after the transient bond breaking and the Maxwell type rheological response is obtained. In the case of the dual crosslink systems, the terminal flow is suppressed by the permanent chemical crosslinks, thus the dynamics of the gels with a small number of transient crosslinks can be measured and studied.

5. Conclusions

In this paper, the dynamics of the PVA-borax dual crosslink hydrogels as a function of the chemical and physical crosslinker concentrations were studied. The constitutive theory which predicts the stress-strain behaviors in both tensile and torsion tests, was used to determine a set of four reduced parameters fitting both tests. The validity of the theory for the PVA dual crosslink gels at various crosslinking ratios was confirmed. To systematically describe the network dynamics and to provide molecular interpretation of the model parameters, we discussed the crosslinkers concentration dependences of the elastic modulus, the characteristic relaxation time and its distribution.

Evidently the main contribution of the transient crosslinkers is the time-dependent elastic population having the elastic modulus of $\mu\bar{\gamma}_{\infty}\frac{t_B}{2-\alpha_B}$, with a large dissipation. With increasing crosslinker concentration, this modulus increases. Besides this transient population of the elasticity which was expected, we found a second population of longer lived elastically active chains, measured as part of the low frequency modulus, $\mu\rho$, but higher than the modulus of the corresponding chemical gel. This additional long live population of crosslinks increases with transient crosslinker concentration and had not been previously identified for the PVA dual crosslink gel. We speculate that these long live crosslinks are due to clustering of mobile transient crosslinkers which can bind to any part of the chain. This result suggests that the dissipative properties of the dual crosslink gels do not proportionally increases with the transient crosslinker concentrations, and formation of such slower population needs to be considered.

It is noteworthy that the concentration of transient crosslinks can influence the relaxation time. We found that the network relaxation time τ_X obtained from the peak of G'' increases with decreasing borax concentration. This crosslinker concentration dependence was interpreted to

be a consequence of an imperfect relaxation of the subchain due to bond reassociation faster than the chain relaxation: before full relaxation of a chain, multiple transient crosslink breaking and healing occur, increasing the apparent relaxation time τ_X. The average length of the subchain between two physical crosslinks is thus a parameter as it determines the Rouse relaxation time.

The scaling analysis with eq.16i,iii,iv suggests that the network relaxation time is inversely proportional to the concentration of the elastically active crosslinks and to the square root of the concentration of available binding sites. The studied dual crosslink gels have plenty of binding sites for the mobile transient crosslinkers on the chains, and at the studied conditions where the binding is far below the saturation, the binding site concentration remains high. This results in a fast bond healing time and very low open transient crosslinker concentration. Thus the dynamics are governed by the change in the total active crosslinker concentration, or by the Rouse relaxation time.

Networks with less binding sites in fixed positions along the chain can be developed, by copolymerizing monomers with and without ligand, for example. Such networks have a lower binding site concentration and saturation can be easily achieved. Close to the saturation the available binding site concentration decreases and concentration of open crosslinks and the bond healing time would increase, resulting in crosslinking ratio dependences of the network dynamics different from the current system. Systematic comparative studies are necessary for complete understanding.

The distribution of the apparent relaxation times, expressed in the theory as the exponent α_B, corresponds to the distribution of the Rouse relaxation time. We showed that the exponent α_B is a function of the number of the relaxation modes on a permanent chain having transient crosslinks, expressed as the ratio of the high frequency modulus and the low frequency modulus,

$N_P = \left(\mu\bar{\gamma}_\infty \cdot \frac{t_B}{2-\alpha_B}\right)/\mu\rho = [G'(\omega \to \infty) - G'(\omega \to 0)]/G'(\omega \to 0)$. We believe that the simple relation between α_B and N_P expressed by eq.17 also proves that the Rouse dynamics of the subchains determine the network relaxation. This result suggests also that the number of the fitting parameter of the constitutive model can be reduced to three, as α_B is a function of the other three parameters.

Supporting Information

Derivation of Equation 11. Fitting curves for tensile and torsion tests for all the dual crosslink gels tested in this work.

Acknowledgements

Jingwen Zhao has benefitted a scholarship from the Chinese Scholarship Council. This project has received funding from the European Research Council (ERC) under the European Union's Horizon 2020 research and innovation program under grant agreement AdG No 695351.

References

(1) Okumura, Y.; Ito, K. The Polyrotaxane Gel: A Topological Gel by Figure-of-Eight Cross-links. *Adv. Mater*. **2001**, 13, 485-487.

(2) Haraguchi, K.; Takehisa, T. Nanocomposite Hydrogels: A Unique Organic–Inorganic Network Structure with Extraordinary Mechanical, Optical, and Swelling/De-swelling Properties, *Adv. Mater*. **2002**, 14, 1120-1124.

(3) Gong, J.-P.; Katsuyama, Y.; Kurokawa, T.; Osada, Y. Double-Network Hydrogels with Extremely High Mechanical Strength. *Adv. Mater*. **2003**, 15, 1155-1158.

(4) Sakai, T.; Matsunaga, T.; Yamamoto, Y.; Ito, C.; Yoshida, R.; Suzuki, S.; Sasaki, N.; Shibayama, M.; Chung, U. Design and Fabrication of a High-Strength Hydrogel with Ideally Homogeneous Network Structure from Tetrahedron-like Macromonomers. *Macromolecules* **2008**, 41, 5379−5384.

(5) Gong, J.-P. Why are double network hydrogels so tough? *Soft Matter* **2010**, 6, 2583-2590.

(6) Lin, W.C.; Fan, W.; Marcellan, A.; Hourdet, D.; Creton, C. Large strain and fracture properties of poly (dimethylacrylamide)/silica hybrid hydrogels. *Macromolecules* **2010**, 43, 2554-2563.

(7) Sun, T.L.; Kurokawa, T.; Kuroda, S.; Ihsan, A.B.; Akasaki, T.; Sato, K.; Haque, M.A.; Nakajima, T.; Gong, J.-P. Physical hydrogels composed of polyampholytes demonstrate high toughness and viscoelasticity. *Nat. Mater*. **2013**, 12, 932-937.

(8) Sun, J.-Y.; Zhao, X.; Illeperuma, R.K.; Chaudhuri, O.; Oh, K.H.; Mooney, D.J.; Vlassak, J.J.; Suo, Z. Highly stretchable and tough hydrogels. *Nature* **2012**, 489, 133-136.

(9) Tuncaboylu, D.C.; Sari, M.; Oppermann, W.; Okay, O. Tough and Self-Healing Hydrogels Formed via Hydrophobic Interactions. *Macromolecules* **2011**, 44, 4997-5005.

(10) Zhang, J.; Wang, N.; Liu, W.; Zhao, X.; Lu, W. Intermolecular hydrogen bonding strategy to fabricate mechanically strong hydrogels with high elasticity and fatigue resistance. *Soft Matter* **2013**, 9, 6331-6337.

(11) Luo, F.; Sun, T.L.; Nakajima, T.; Kurokawa, T.; Zhao, Y.; Ihsan, A.B.; Guo, H.; Li, X.F.; Gong, J.-P. Crack Blunting and Advancing Behaviors of Tough and Self-healing Polyampholyte Hydrogel. *Macromolecules* **2014**, 47, 6037–6046.

(12) Taylor, D.L.; in het Panjuis, M. Self-Healing Hydrogels. *Adv. Mater*. **2016**, 28, 9060-9093.

(13) Xu, Z.; Li, J.; Gao, G.; Wang, Z.; Cong, Y.; Chen, J.; Yin, J.; Nie L.; Fu, J. Tough and self-recoverable hydrogels crosslinked by triblock copolymer micelles and Fe^{3+} coordination. *J. Polym. Sci. B* 2018, **56**, 865–876.

(14) Narita, T.; Mayumi, K.; Ducouret, G.; Hébraud, P. Viscoelastic Properties of Poly(vinyl alcohol) Hydrogels Having Permanent and Transient Cross-Links Studied by Microrheology, Classical Rheometry, and Dynamic Light Scattering. *Macromolecules* **2013**, 46, 4174–4183.

(15) Mayumi, K.; Marcellan, A.; Ducouret, G.; Creton, C.; Narita, T. Stress–Strain Relationship of Highly Stretchable Dual Cross-Link Gels: Separability of Strain and Time Effect. *ACS Macro Lett.* **2013**, 2, 1065–1068.

(16) Zhao, J.; Mayumi, K.; Creton, C.; Narita, T. Rheological properties of tough hydrogels based on an associating polymer with permanent and transient crosslinks: Effects of crosslinking density *J Rheol*, **2017**, 61, 1371-1383.

(17) Guo, J.; Liu, M.L.; Zehnder, A.T.; Zhao, J.; Narita, T.; Creton, C.; Hui, C.Y. Fracture mechanics of a self-healing hydrogel with covalent and physical crosslinks: A numerical study. *J. Mech. Phys. Solids* **2018**, 120, 79-95.

(18) Long, R.; Mayumi, K.; Creton, K.; Narita, T.; Hui, C.Y. Time Dependent Behavior of a Dual Cross-Link Self-Healing Gel: Theory and Experiments. *Macromolecules* **2014**, 47, 7243-7250.

(19) Long, R.; Mayumi, K.; Creton, C.; Narita, T.; Hui, C.Y. Rheology of a dual crosslink self-healing gel: Theory and measurement using parallel-plate torsional rheometry. *J. Rheol.* **2015**, 59, 643-665.

(20) Guo, J.; Long, R.; Mayumi, K.; Hui, C.Y. Mechanics of a dual cross-link gel with dynamic bonds: steady state kinetics and large deformation effects. *Macromolecules* **2016**, 49, 3497–3507.

(21) Mayumi, K.; Guo, J.; Narita, T.; Hui, C.Y.; Creton, C. Fracture of dual crosslink gels with permanent and transient crosslinks *Extreme Mech. Lett.* **2016**, 6, 52-59.

(22) Liu, M.; Guo, J.; Hui, C.-Y.; Creton, C.; Narita, T.; Zehnder, A., Time-temperature equivalence in a PVA dual cross-link self-healing hydrogel. *J. Rheol.* **2018**, 62, 991-1000.

(23) C_{closed} is the concentration of the borate ions absorbed and bound to the chemical gel, and C_{borax} is the borax concentration in the feed of the solution in which the chemical gel is immersed. The ratio of the volume of the solution to that of the chemical gel is 20 and the gel volume was kept constant, thus borate ion can be concentrated in the gel and C_{closed} can be larger than C_{borax}, up to about 20 times.

(24) Kean, Z.S.; Hawk, J.L.; Lin, S.; Zhao, X.; Sijbesma, R.P.; Craig, S.L. Increasing the maximum achievable strain of a covalent polymer gel through the addition of mechanically invisible cross-links. *Adv. Mater.* **2014**, 26, 6013-6018.

(25) Pezron, E.; Leibler, L.; Ricard, A.; Lafuma, F.; Audebert, R. Complex Formation in Polymer-Ion Solutions. 1. Polymer Concentration Effects, *Macromolecules* **1989**, 22, 1169–1174.

(26) Pezron, E.; Leibler, L.; Lafuma, F. Complex Formation in Polymer-Ion Solutions. 1. Polyelectrolyte Effects, *Macromolecules* **1989**, 22, 2656–2662.

(27) Above a polymer concentration C_l at which the blob size ξ_l is in the order of the size of loop formed by intrachain crosslink, interchain crosslinking should become favored. Thus the ratio of interchain crosslinks to intrachain crosslinks, $R_{inter/intra}$, scales with the blob size ξ as $R_{inter/intra} \approx \xi_l/\xi$. Since ξ varies with the polymer concentration C as $\xi \sim C^{-5/4}$, we have $R_{inter/intra} \approx (C/C_l)^{5/4}$. Pezron et al. reported C_l of 8 wt% for PVA.

(28) Sinton, S.W. Complexation chemistry of sodium borate with poly(vinyl alcohol) and small diols: a boron-11 NMR study. *Macromolecules* **1987**, 20, 2430 – 2441.

(29) Huang, G.; Zhang, H.; Liu, Y.; Chang, H.; Zhang, H.; Song, H.; Xu, D.; Shi, T. Strain Hardening Behavior of Poly(vinyl alcohol)/Borate Hydrogels. *Macromolecules* **2017**, 50, 2124–2135.

(30) The concentration of OH groups in the chemical gel is about 2.73 M for the PVA concentration of 12 w%, thus the concentration of the binding site for diol complexation with borate ions (and with the chemical crosslinker glutaraldehyde) is C_0 = 1.36 M.

(31) Indei, T.; Takimoto, J., Linear viscoelastic properties of transient networks formed by associating polymers with multiple stickers, *J. Chem. Phys*. **2010**, 133, 194902-194914.

(32) Doi, M.; Edwards, S.F., *The Theory of Polymer Dynamics*, Clarendon, Oxford, 1986.

(33) Li, H.; Zhang, W.; Zhang, X.; Shen, J.; Liu, B.; Gao, C.; Zou, G. Single molecule force spectroscopy on poly(vinyl alcohol) by atomic force microscopy. *Macromol. Rapid Commun.* **1998**, 19, 609−611.

(34) At equilibrium, the transient bond breaking rate (M s^{-1}) is the same as the transient bond healing rate, $k_{break} \cdot C_{di} = k_{heal} \cdot C_{site} \cdot C_{open}$, where k_{break} (s^{-1}) is the breaking rate constant and k_{heal} (M^{-1} s^{-1}) is the healing rate constant. The binding constant K_2 (M^{-1}) is equivalent to the ratio of the healing rate constant to the breaking rate constant, $K_2 = \frac{k_{\mathrm{heal}}}{k_{\mathrm{break}}}$. Since we can define the breaking time t_B as $t_b = \frac{1}{k_B}$, and the healing time t_H as $t_H = \frac{1}{k_H \cdot C_{\mathrm{site}}}$, we have $\frac{t_B}{t_H} = \frac{k_H \cdot C_{\mathrm{site}}}{k_B} = K_2 \cdot C_{\mathrm{site}} = \frac{C_{di}}{C_{\mathrm{open}}}$.